Available online at www.sciencedirect.com

ScienceDirect

Procedia Computer Science 70 (2015) 76 – 84

Procedia Computer Science

4th International Conference on Eco-friendly Computing and Communication Systems

Wavelet Packet Texture Descriptors based four-class BIRADS Breast Tissue Density Classification

Indrajeet Kumar[a], H S Bhadauria[b], *Jitendra Virmani[c]

[a,b]G.B. Pant Engineering College, Pauri Garhwal, UK, India-246194.

[c]Thapar University- Patiala, Punjab, India- 147004

Abstract

The present work proposes a computer aided diagnostic (CAD) system for four-class BIRADS breast tissue density classification. The study has been carried out on a total of 480 mammograms taken from the DDSM database. The ROI has been extracted manually from each image. Each ROI has been decomposed up to 2nd level of decomposition using wavelet packet transform, resulting in 16 sub-band images for each ROI image. From each sub-band image three multi-resolution texture descriptors (i.e., mean, standard deviation and energy descriptors) are computed , resulting in texture feature vector of length 48 (16 X 3) for each ROI. The results obtained from the present work, indicate that the standard deviation and energy descriptors computed from sub-band images obtained by using wavelet packet transform with haar wavelet filter yield the highest overall classification accuracy of 73.7 % for four-class breast tissue density classification. Thus it can be concluded that standard deviation and energy multi-resolution texture descriptors computed from sub-band images yielded by wavelet packet transform using haar wavelet filter contain significant information for differential diagnosis between four BIRADS breast tissue density classes.

Peer-review under responsibility of the Organizing Committee of ICECCS 2015

Keywords: Mammography; Breast tissue density; wavelet packet transform; Multi-resolution analysis; Support vector machine (SVM); Wavelet packet texture descriptor.

1. Introduction

Breast tissue density[1] is a strong and consistent factor for indicating the development of breast cancer among women across the world. It is the most common life threatening form of cancer[2] that is found in women after the vaginal cancer. Early detection of breast tumor is really a challenging task even for the experienced radiologists due to the fact that sometimes these lesions are masked by the dense texture pattern exhibited by mammographic images.

* Jitendra Virmani. Tel.: +91-8427593840; fax: +91-175-2364498..

E-mail address: [a]erindrajeet@gmail.com, [c]jitendra.virmani@gmail.com, [b]*hsb76iitr@gmail.com*

Peer-review under responsibility of the Organizing Committee of ICECCS 2015
doi:10.1016/j.procs.2015.10.042

In 1977 Wolfe[1] presented the association between breast tissue density patterns and the possibility of the risk of developing breast cancer. Fundamentally, classification of different breast tissue density patterns is carried out by visual analysis of the relative amounts of fibro-glandular tissues versus fatty tissues present in the breast.

The appearance[3] of the different tissues reflects different intensity; darker region indicates fatty tissue while brighter region represents dense tissues on mammograms. According to BIRADS breast tissue density classification, the tissue density can be classified into four-classes i.e., BIRADS-I: entirely fatty, BIRADS-II: some fibro-glandular tissue, BIRADS-III: heterogeneously dense tissue and BIRADS-IV: extremely dense. The BIRADS breast tissue density classification is easier in case of *typical cases* where clear distinction can be made between amounts of fibro-glandular tissues present in the mammographic image. However, it has been observed that in atypical cases, where there is significant overlap in terms of visual appearance between images belonging to different classes, the differential diagnosis between different BIRADS breast tissue density classes can be considerably difficult.

Development of CAD system for classification of breast tissue density is clinically significant because of two reasons, i.e., (*1*) increase in breast tissue density is associated with risk of breast cancer and (*2*) the differential diagnosis between different breast tissue density classes is considerably difficult specifically for atypical cases. Accordingly there has been significant interest in the research community to develop CAD[4] systems for prediction of breast tissue density. The CAD systems proposed in the literature for breast tissue density classification can be divided into two categories, i.e., (*1*) CAD systems designed using segmented breast tissue (SBT) obtained after removal of pectoral muscle and background elimination and (*2*) CAD systems designed using regions of interest (ROIs) of different sizes. The brief description of the studies carried out for breast tissue density classification is shown in Table 1.

Table 1. Brief overview of different studies carried out on different mammographic image databases for four-class classification

Author(s), Year	Segmented Breast Tissue/ROI	No. of images	Name of Database	Classifier	Considered class	Accuracy (%)
Karssemeijer[5] , 1998	SBT	615	Nijmegen	KNN	4-class	65.0
Bovis[6], 2002	SBT	144	DDSM	ANN	4-class	71.4
Oliver[7], 2005	SBT	615	DDSM	KNN, Decision tree	4-class	47.0
Oliver[7], 2005	SBT	270	MIAS	KNN	4-class	67.0
				Decision tree	4-class	73.0
Bosch[8], 2006	SBT	2052	DDSM	KNN, SVM	4-class	84.7
Bosch[8], 2006	SBT	322	MIAS	KNN, SVM	4-class	95.4
Oliver[9], 2008	SBT	132	DDSM	SFS+KNN	4-class	77.0
Oliver[9], 2008	SBT	322	MIAS	SFS, KNN	4-class	66.0
Oliver[10], 2010	SBT	88	DDSM	LDA-PCA	2-class	79.0
Liu[11], 2011	ROI	88	T.T. Hospital	SVM	4-class	86.4
Qu[12], 2011	SBT	322	MIAS	E-FELM	4-class	72.6
Z. Chen[13], 2011	SBT	322	MIAS	KNN, Bayesian	4-class	75.0
M. Mustra[14], 2012	ROI	144	MIAS	KNN (k=1)	4-class	79.2
Masmoudi[15], 2013	SBT	2052	EL FARABI	KNN	4-class	79.0

Note: - SBT: Segmented breast tissue; ROI: Region of interest; 4-Class: BIRADS-I, BIRADS-II, BIRADS-III and BIRADS-IV breast tissue density classification; 2-class: Fatty and dense breast tissue density classification. The studies carried out on DDSM database for four-class breast tissue density classification are highlighted with gray background.

It is worth mentioning that extraction of SBT from original mammogram requires additional steps, i.e. background elimination and removal of pectoral muscle which are time consuming on the other hand extraction of fixed size ROIs from the original mammogram is significantly simpler. It has been ascertained in few studies[16] that the density information is maximum at the center of the breast tissue behind the nipple. Accordingly, in the present work, ROIs of size 128 × 128 pixels are extracted from the center of each mammogram and the multi-resolution

texture descriptors i.e. standard deviation and energy descriptors are computed from the 16 sub-band images obtained by decomposing each ROI image using wavelet packet transform. The SVM classifier has been used for classification of mammographic images into four density classes as per BIRADS categories. For evaluating the effectiveness of the proposed algorithm, images are taken from the benchmark database Digital database of screening mammograms[17] (DDSM).

The present work can be directly compared with only four studies[6-10] reporting four-class BIRADS breast tissue density classification using DDSM database. However it can be observed that the maximum classification accuracy of 84.7 % and the minimum classification accuracy of 47 % have been achieved for four-class BIRADS breast tissue density classification using SBT on DDSM database. The present work is the first attempt to design a CAD system for four-class BIRADS breast tissue density classification using fixed size ROI extracted from the center of the breast tissue. A brief description of related studies for four-class BIRADS breast tissue density classification carried out on MIAS benchmark database and databases collected by individual research groups is also given in table 1.

In clinical practice four-class breast tissue density classifications is carried out by the radiologist by visual analysis of texture patterns of the center region of the breast tissue based on their expertise. It has been shown in several studies that texture description can be carried out efficiently in transform domain. Accordingly in the present work, a four-class breast tissue density classification has been carried out using multi-resolution transform domain texture descriptors.

2. Material and Methods

2.1. Database description

In this present work, a total of 480 (120 × 4) mammograms (MLO views) comprising of 120 mammograms from each of the 4 ACR-BIRADS (BIRADS-I to BIRADS-IV) breast tissue density classes were taken from the DDSM [17] database. The DDSM database is a standard bench mark database in which the expert evaluation for breast tissue density classification with respect to ACR-BIRADS standard is specified for each image. The brief description of the dataset used in the present work and its further partioning into training and testing data is shown in Fig. 1.

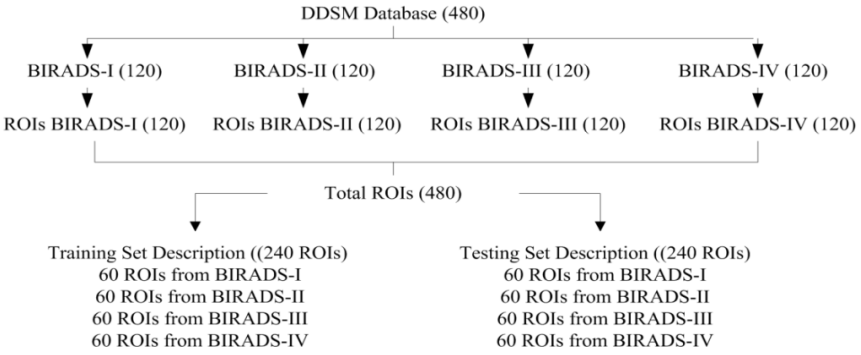

Fig. 1. Database description

From Fig. 1, it can be observed that the training and testing dataset consist of 60 ROIs images from each of the four BIRADS breast tissue density classes.

2.2 Proposed CAD System

The block diagram of the proposed CAD system for four-class breast tissue density classification as per BIRAS standard is shown in Fig. 2. To implement the proposed CAD system design, 480 MLO view mammograms are taken from the DDSM database and ROIs of size 128 × 128 pixels are extracted from the center of each mammogram. Each ROI image is decomposed up to second level by 2-D wavelet packet transformation[18] (2D-

WPT), resulting in 16 sub-band feature images (FIs) of each ROI. The multi-resolution texture descriptors i.e., mean, standard deviation and energy features are extracted from all the 16 sub-band feature images obtained for each ROI image. In classification module, support vector machine (SVM) is used as a classifier.

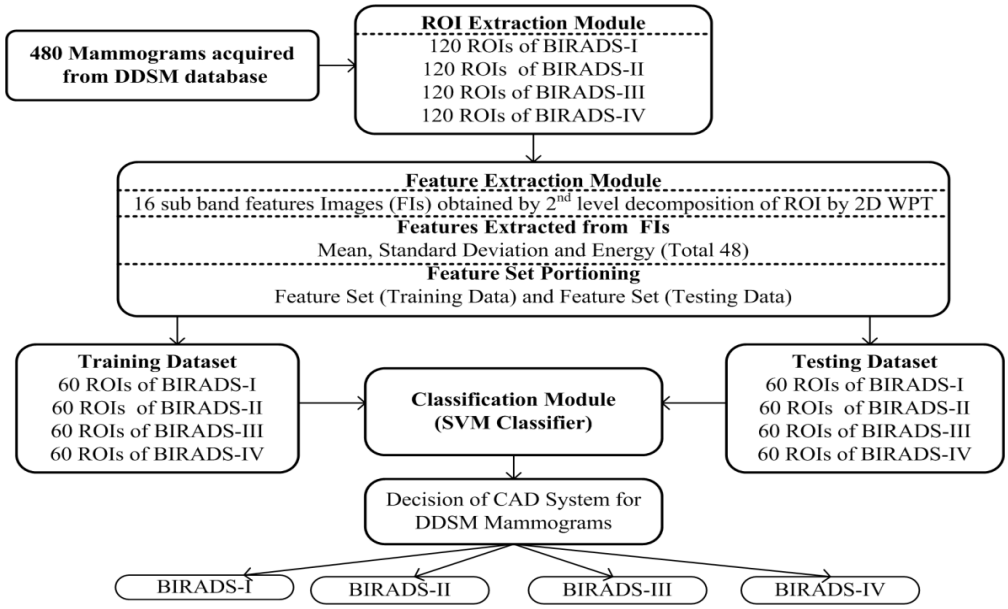

Fig. 2. Proposed CAD System

The CAD system consists of mainly three modules: (*1*) ROI extraction module (*2*) feature extraction module and (*3*) classification module. The brief description of each module is given below.

2.2.1 Region of Interest (ROI) Extraction Module

During routine clinical practice, the radiologist visualise the center of breast tissue for differential diagnosis between different classes of breast tissue density. The experimental study carried out by Li[16] indicates that the texture pattern of the center of the breast tissue behind the nipple provides maximum information of tissue density. Accordingly, in the present work ROIs of size 128 x 128 are manually extracted from the center of the breast and behind the nipple for each mammogram as shown in Fig. 3.

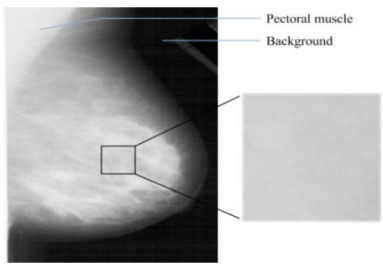

Fig. 3. ROI extraction module.

2.2.2 Feature Extraction Module

Feature extraction in transform domain can be carried out using multi-resolution schemes[18-19] such as stationary wavelet transforms (SWT), discrete wavelet transform (DWT) and wavelet Packet transforms (WPT). In 2D-DWT lower frequency sub-image is recursively decomposed; which may not be efficient for the texture description, because most of the texture information appears in the middle and high frequency channels. Therefore in the present work multi-resolution texture descriptors are computed from 16 sub-band images obtained after second level decomposition of each ROI image by using 2D WPT with various compact support wavelet filters. It has been demonstrated in various studies that the efficient description of texture depends upon the properties of the wavelet filter. Thus in the present work ten different compact support wavelet filters including db1, db4, db6, bior3.1, bior3.3, bior4.4, sym3, sym5, coif1 and coif2 have been used to obtain sub-band images for each ROI image in order to obtain the best wavelet filter for the present task of four-class BIRADS breast tissue density classification. The important properties of these compact support wavelet filters are given in table 2.

Table 2. Properties of wavelet filters

	Daubechies			Biorthogonal			Symlets		Coiflets	
	haar #	db4	db6	bior3.1	bior3.3	bior4.4	sym3	sym5	coif 1	coif 2
Bi-orthogonal	No	No	No	Yes	Yes	Yes	No	No	No	No
Orthogonal	Yes	Yes	Yes	No	No	No	Yes	Yes	Yes	Yes
Symmetry	Yes	No	No	Yes	Yes	Yes	No	No	No	No
Asymmetry	No	Yes	Yes	No	No	No	No	No	No	No
Near symmetry	No	No	No	No	No	No	Yes	Yes	Yes	Yes
Compact support	Yes	Yes	Yes	Yes	Yes	Yes	Yes	Yes	Yes	Yes

Note: Haar# is also known as Db1 wavelet filter.

2.2.2.1 Wavelet packet texture descriptors

In last few years transform domain multi-resolution techniques[18-19] have been extensively used for description of texture in medical images. In the present work mean, standard deviation and energy multi-resolution texture descriptors have been computed from all the 16 sub-band feature images resulting from 2D level decomposition of each ROI image.

$$Mean = \left(\frac{1}{MxN} \sum_{X=1}^{M} \sum_{Y=1}^{N} \left| SI_j(X,Y) \right| \right) \tag{1}$$

$$Std_j = \left(\frac{1}{MxN} \sum_{X=1}^{M} \sum_{Y=1}^{N} \left| SI_j(X,Y) - Mean_j \right|^2 \right)^{1/2} \tag{2}$$

$$Energy_j = \frac{1}{MxN} \sum_{X=1}^{M} \sum_{Y=1}^{N} \left| SI_j(X,Y) \right|^2 \tag{3}$$

Here SI_j are sub-image of size M × N at level j=1, 2, 3...7. In this work size of ROI is 128 × 128 pixels, therefore level of decomposition is up to seven.

2.2.3 Classification Module

The classification capability of classifier is tested with the instances of feature vector which are not used for the train the classifier. The data used in this work consist of total 480 ROIs, which are taken from 120 ROIs of each

BIRADS class mammograms. These dataset are further classified into training and testing instance of dataset which consist of 240 ROIs; 60 ROIs from each BIRADS breast tissue density class. A complete description of used dataset for this study is shown in Fig. 1. For the present work support vector machine[20-22] (SVM) is used as classifier by importing *LibSVM*[20] library files. For the evaluation of classification performance overall classification accuracy (OCA) is calculated, which is ratio of the number of correctly classified ROIs over the total number of actual ROIs. For the individual class classification, individual class classification accuracy abbreviated as $ICA_{class\ name}$ is evaluated by the correctly classified ROIs over the total number of ROIs of this particular class.

3. Results and discussion

Initially, all possible texture descriptor feature vectors (TDFVs), shown in table 3, (resulting from individual mean, standard deviation and energy descriptors and combined TDFVs resulting from combinations of mean, standard deviation and energy descriptors computed from each of the 16 sub-band feature images resulting from 2nd level decomposition of each ROI image using 2D-WPT with ten different wavelet filters) are computed. Support vector machine classifier is used to compare the capability of these TDFVs for efficient texture description by different wavelet filters for four-class BIRADS breast tissue density classification. The maximum and minimum classification accuracy obtained by all TDFVs is reported in table 3 with the corresponding wavelet filter. From table 3, it is observed that haar wavelet filter gives maximum accuracy for all possible TDFVs. The highest accuracy of 73.7 % is obtained from haar filter using standard deviation and energy TDFV (highlighted with gray background in table 3).

Table 3. Comparative analysis of performance of wavelet packet filters for all TDFVs using SVM classifier.

TDFVs	L	Max. Acc.	Wavelet filter	Min. Acc.	Wavelet filter
mean	16	65.0	haar	55.4	sym3
standard deviation (SD)	16	59.1	haar	46.2	bior3.1
energy	16	65.0	haar	51.2	bior3.3
mean+SD	32	71.2	haar	64.1	db4
mean+energy	32	65.0	haar	53.7	bior3.3
SD+energy	**32**	**73.8**	**haar**	64.3	db4
mean+SD+energy	48	70.0	haar	61.7	sym3, db4, bior3.3

Note that for all seven TDFVs maximum accuracy is obtained by using Haar wavelet filter. However, the highest accuracy of 73.7 % (indicated in bold) is obtained by using Haar wavelet filter with SD+energy TDFV of length 32. Accuracy values are expressed in percentage. TDFVs: Texture descriptor feature vectors; L: Length of TDFV; SD: Standard deviation.

From table 3, it can be observed that the maximum classification accuracy of 73.7 % is obtained using haar wavelet filter with combination of standard deviation and energy texture descriptor. On the other hand minimum accuracy of 49.0 % is obtained using bior4.4 wavelet filter with standard deviation texture descriptor.

In the next experiment, individual TDFVs, i.e. mean, standard deviation and energy TDFVs using haar wavelet filter are considered for four-class BIRADS breast tissue density classification. The classification accuracy of SVM classifier obtained for individual TDFVs using haar filter is summarised in table 4.

Table 4. The classification results of SVM obtained for mean ,standard deviation and energy TDFVs using haar wavelet filter

TDFVs		CM				Accuracy (%)				
		B-I	B-II	B-III	B-IV	OCA	ICA_{B-I}	ICA_{B-II}	ICA_{B-III}	ICA_{B-IV}
mean	B-I	40	19	1	0					
	B-II	20	32	7	1	65.0	**66.6**	53.3	48.3	91.6
	B-III	2	15	29	14					
	B-IV	0	0	5	55					

standard deviation	B-I	39	10	5	6					
	B-II	9	33	13	5	59.1	65.0	**55.0**	37.6	80.0
	B-III	5	15	22	18					
	B-IV	9	0	3	48					
energy	B-I	42	17	1	0					
	B-II	20	29	10	1	**65.0**	**70.0**	48.3	**48.3**	**93.3**
	B-III	3	14	29	14					
	B-IV	0	1	3	56					

Note:- CM: Confusion Matrix, TDFVs (16): Texture descriptor feature vectors of length 16 ; OCA: Overall classification accuracy; $ICA_{B\text{-}I}$: Individual classification accuracy for BIRADS-I; $ICA_{B\text{-}II}$: Individual classification accuracy for BIRADS-II; $ICA_{B\text{-}III}$: Individual classification accuracy for BIRADS-III; $ICA_{B\text{-}IV}$: Individual classification accuracy for BIRADS-IV; B-I: BIRADS-I ; B-II: BIRADS-II; B-III: BIRADS-III; B-IV: BIRADS-IV.

It can be easily observed from table 4 that the maximum classification accuracy of 65 % is obtained in case of energy TDFV of length 16. Individual classification accuracy of 93.3 % is achieved for BIRADS-IV, 70 % for BIRADS-I and 48.3 % for BIRADS-III from energy TDFV. An accuracy of 55 % is achieved for BIRADS-II from standard deviation TDFV.

In next experiment, classification results of SVM classifier for combined TDFVs consisting of combinations of mean, standard deviation and energy texture descriptors using haar wavelet filter are summarized in table 5.

Table 5. The classification results of SVM classifier for combination of Energy, Standard deviation and Mean TDFVs using haar wavelet filter

TDFVs		CM				Accuracy (%)				
		B-I	B-II	B-III	B-IV	OCA	$ICA_{B\text{-}I}$	$ICA_{B\text{-}II}$	$ICA_{B\text{-}III}$	$ICA_{B\text{-}IV}$
mean+SD	B-I	43	15	2	0					
(32)	B-II	16	39	4	1	71.2	71.6	65.0	52.6	96.6
	B-III	1	13	31	15					
	B-IV	0	0	2	58					
mean+energy	B-I	41	17	2	0					
(32)	B-II	20	33	6	1	65.0	68.3	55.0	46.6	90.0
	B-III	2	16	28	14					
	B-IV	0	0	6	54					
SD+energy	B-I	45	14	1	0					
(32)	B-II	14	41	4	1	**73.7**	**75.0**	**68.3**	**55.0**	**96.6**
	B-III	1	13	33	13					
	B-IV	0	0	2	58					
mean+SD+energy	B-I	42	16	2	0					
(48)	B-II	17	39	3	1	70.0	70.0	65.0	48.3	96.6
	B-III	1	14	29	16					
	B-IV	0	0	2	58					

Note:- CM: Confusion Matrix, TDFVs: Texture descriptor feature vectors; L: Length of TDFVs; SD: Standard deviation; OCA: Overall classification accuracy; $ICA_{B\text{-}I}$: Individual classification accuracy for BIRADS-I; $ICA_{B\text{-}II}$: Individual classification accuracy for BIRADS-II; $ICA_{B\text{-}III}$: Individual classification accuracy for BIRADS-III; $ICA_{B\text{-}IV}$: Individual classification accuracy for BIRADS-IV; B-I: BIRADS-I ; B-II: BIRADS-II; B-III: BIRADS-III; B-IV: BIRADS-IV.

From table 5, it is observed that maximum accuracy of 73.7 % achieved for TDFV using standard deviation and energy as mentioned in row 3 of Table 5. When combination of Mean and standard deviation are considered then obtained accuracy is 71.2 % which is the second highest accuracy. Similarly, 65 % of accuracy is achieved for the combination of mean and energy texture features. Same features are carried forward for further analysis and the obtained accuracy is 70 % after combining all feature vectors (length 48), which is less than the best accuracy of the proposed CAD system.

4. Conclusion

Early detection of breast tissue density always helps radiologist for better management of the disease and adequate scheduling of treatment options. Therefore, the experiments carried out in this work a CAD system for classification of breast tissue density as per BIRADS standard have been developed by multi-resolution texture analysis of DDSM mammographic images by using ten compact support wavelet filter. The proposed CAD system achieves an overall classification accuracy of 73.7 % using the combined TDFV consisting of standard deviation and energy descriptors. The proposed system yields ICA values of 75%, 68.3%, 55% and 96.6% for BIRADS-I, BIRADS-II, BIRADS-III and BIRADS-IV classes respectively.

References

1. Wolfe J.N. Risk for Breast Cancer Development Determined by Mammographic Parenchymal Pattern, *Cancer*, Vol. 37, No. 5, May 1977; pp. 2486-2492.
2. American cancer society. *Breast Cancer Early Detection The importance of finding breast cancer early*, Copyright American Cancer Society, 2013 last reviewed 2014.
3. Astley S.M., Brady M., Rose C., Zwiggelaar R. Digital Mammography, *Proceedings of 8th International Workshop, IWDM 2006 Manchester*, UK, June 18-21, 2006.
4. Kumar I., Virmani J., Bhadauria H.S. A review of breast density classification methods", In: *Proceeding of Indiacom-2015*; © IEEE 978-9-3805-4416-8/15/$31.00.
5. Karssemeijer N. Automated classification of parenchymal patterns in mammograms, *Physics in Medicine and Biology,* Vol. 43, No. 2, 1998; pp.365-389.
6. Bovis K., Singh S. Classification of mammographic breast density using a combined classifier paradigm, In *medical image understanding and analysis (MIUA) conference,* Portsmouth, (C), 2002; pp. 1–4.
7. Oliver A., Freixenet J., Zwiggelaar R., Automatic classification of breast density, In *Proceedings of the IEEE International Conference on Image Processing*, ICIP 2005, Vol. 2, Genova, September, 2005; pp. 1258-1261.
8. Bosch A., Munoz X., Oliver A., Marti J. Modelling and classifying breast tissue density in mammograms, In *Proceedings of the 2006 IEEE Computer Society Conference on Computer Vision and Pattern Recognition (CVPR'06)*, New York, Vol. 2, 2006; pp. 1552-1558.
9. Oliver A., Freixenet J., Marti R., Pont J., Perez E., Denton E.R.E., Zwiggelaar R. A novel breast tissue density classification methodology, *IEEE Transactions on Information Technology in Biomedicine*, Vol. 12, Issue 1, January 2008; pp. 55-65.
10. Oliver A., Llado X., Perez E., Denton E.R.E., Pont J., Freixenet J., Marti J. A statistical approach for breast density segmentation, *Journal of Digital Imaging,* Vol. 23, No 5, October, 2010; pp. 527-537.
11. Liu Q., Liu L., Tan Y., Wang J., Ma X., Ni H. Mammogram density estimation using sub-region classification, In *Proceedings of 4th International Conference on Biomedical Engineering and Informatics (BMEI)*, Shanghai, October 2011; pp. 356-359.
12. Qu Y., Shang C., Shen Q., "Evolutionary fuzzy extreme learning machine for mammographic risk analysis", *International Journal of Fuzzy Systems,* Vol. 13, No. 4, 2011; pp. 282-291.
13. Chen Z., Denton E., Zwiggelaar R. Local feature based mammographic tissue pattern modelling and breast density classification, In *Proceedings of 4th International Conference on Biomedical engineering and Informatics,* Shanghai, October 2011; pp. 351-355, 15-17.
14. Mustra M., Grgic M., Delac K. Breast density classification using multiple feature selection, *AUTOMATIKA, Journal for Control, Measurement, Electronics, Computing and Communication,* Vol. 53, No. 4, 2012; pp. 362–372.
15. Masmoudi A.D., Ayed N.G.B., Maasmoudi D.S., Abid R. LBPV descriptors-based automatic ACR/BIRADS classification approach, *EURASIP Journal on Image and Video Processing,* Vol. 2013, No. 1, April 2013; pp. 1-9.
16. Li H., Giger M.L., Huo Z, Olopade O.I., Lan L., B.L., Bonta I. Computerized analysis of mammographic parenchymal patterns for assessing breast cancer risk: Effect of ROI size and location, *Medical Physics 31*, 549; 2004; doi: 10.1118/1.1644514.
17. Heath M., Bowyer K., Kopans D., Moore R., and Kegelmeyer P. J. The digital database for screening mammography, in *Proc. Int. Workshop Dig. Mammography*, 2000, pp. 212–218.
18. Virmani J., Kumar V., Kalra N. and Khandelwal N. SVM-based characterization of liver ultrasound images using wavelet packet texture descriptors, *Journal of Digital Imaging*, Vol. 26, No. 3, October 2012; pp. 530-543.
19. Virmani, J., Kriti. Breast Tissue Density Classification Using Wavelet-Based Texture Descriptors. *Proceedings of the Second International Conference on Computer and Communication Technologies* (IC3T-2015, Vol-3); pp. 539-546.

20. Chang CC. *LIBSVM*, A library of support vector machines, Software available at http://www.csie.ntu.edu.tw /~cjlin/libsvm, March, 2012.
21. Virmani J., Kumar V., Kalra N., Khandelwal N. Characterization of primary and secondary malignant liver lesions from B-mode ultrasound, Journal of Digital Imaging, Vol. 26, No. 6, February 2013; pp.1058-1070.
22. Kriti, Virmani, J., Dey, N., Kumar, V. PCA-PNN and PCA-SVM based CAD Systems for Breast Density Classification. In: Hassanien, A.E., et al. (eds.) Applications of Intelligent Optimization in Biology and Medicine. vol. 96, 2015, pp. 159-180.Optimization in Biology and Medicine. vol. 96, 2015, pp. 159-180.